Electrical Conductivity of Aqueous Salt-Free Concentrated Suspensions. Effects of Water Dissociation and CO_2 Contamination

Félix Carrique*,† and Emilio Ruiz-Reina‡

Departamento de Física Aplicada I, Universidad de Málaga, Campus de Teatinos, 29071, Málaga, Spain, and Departamento de Física Aplicada II, Universidad de Málaga, Campus de El Ejido, 29071, Málaga, Spain

Received: May 12, 2009; Revised Manuscript Received: June 2, 2009

In this paper we explore the effects of water dissociation and CO_2 contamination on the electrical conductivity of salt-free concentrated suspensions in static electric fields. The conductivity model here presented is based on a new description of the equilibrium double layer for particles in "realistic" salt-free suspensions recently developed by the authors to account for the latter effects (Ruiz-Reina, E.; Carrique, F. *J. Phys. Chem. B* **2008**, *112*, 11960). It was shown that in most of the cases the neglecting of those effects would lead to a very poor description of common salt-free suspensions, especially, but not only, if the suspensions have been in contact with air. As shown in this paper, the presence of only water dissociation ions suffices to provoke very important changes in the standard salt-free predictions. A realistic aqueous salt-free suspension consists of an aqueous suspension without any electrolyte added during the preparation but including the following ionic species: (i) the "added counterions" stemming from the particle charging process that counterbalance their surface charge (with just this ionic species, the suspension can be considered as an ideal or pure salt-free one), (ii) the H^+ and OH^- ions from water dissociation, and (iii) the ions produced by the atmospheric CO_2 contamination. The model is based on the classical Poisson−Boltzmann theory, the appropriate local chemical reactions, the standard electrokinetic equations, and the cell model approximation to account for electrohydrodynamic particle−particle interactions. Thus, we have studied the electrical conductivity of such realistic salt-free suspensions for different particle volume fraction ϕ and surface charge density σ, and compared it with results of pure salt-free conductivity predictions. The numerical results have shown that water dissociation ions and/or CO_2 contamination has an extreme influence on the suspension conductivity values at low−moderate particle volume fractions. In these situations the role of the added counterions is screened by the other ionic species. Even if the suspensions have not been exposed to the atmosphere, the quantitative changes in conductivity at low volume fractions associated with the presence of water dissociation ions over the added counterions are enormous. It is concluded that it is necessary to take into account the water dissociation influence for ϕ lower than approximately $10^{-2}-10^{-3}$, whereas the atmospheric CO_2 contamination is not negligible if $\phi < 10^{-1}-10^{-2}$, depending on the particle charge. The present work sets the basis for further theoretical models concerning, particularly, the dynamic electrophoresis and dielectric response of such systems.

Introduction

Salt-free colloidal suspensions are nowadays being revised with a renovated interest.[1−13] The term "salt-free" means that only the ions stemming from the charging process of the colloidal particles, which are known as "added counterions", are present in the solution, thus preserving the electroneutrality, and no external salt is added at all. In the recent past, different topics with ideal or pure salt-free suspensions have been explored, for example, the relationship between surface potential and surface charge density,[3,4] the counterion condensation phenomenon,[3,4,9] static[9] and dynamic[12] electrokinetic responses, dielectric response,[13] electroviscous effect,[8] and the renormalization charge.[14]

The study of the counterion condensation effect by using a cell model concept was explored in the 1980s by Alexander et al.[14] and extended more recently with the inclusion of chemical surface reactions for the generation of the particle charge.[15] No considerations regarding particle charge mechanisms like surface group dissociation studies, such as that by Palberg et al.,[16] will be dealt with in this work. Other works concerning counterion condensation with charge regulation have been more recently published by Belloni[17] and Levin.[18] From the experimental point of view, counterion condensation was shown early in the 1990s by Bucci et al.[19] Our treatment adds to a pure salt-free suspension very-well-known chemical reactions in solution related to water and carbonic acid dissociations, with the latter originating from dissolved carbon dioxide in water. A salt-free suspension that includes such effects will be called a realistic salt-free suspension hereafter.

In analogy with the case of suspensions in salt solutions, a Debye length κ^{-1} characterizing the width of the electric double layer (EDL) in a pure salt-free suspension, has been proposed in the literature:[20]

$$\kappa^2 = \frac{e^2 \bar{n}_c z_c^{\,2}}{\varepsilon_0 \varepsilon_{rs} k_B T} = \frac{-3ez_c}{\varepsilon_0 \varepsilon_{rs} k_B T a} \sigma \frac{\phi}{1-\phi} \qquad (1)$$

where e is the elementary electric charge, k_B is the Boltzmann constant, T is the absolute temperature, ε_{rs} is the relative

* Corresponding author. E-mail: carrique@uma.es.
† Departamento de Física Aplicada I.
‡ Departamento de Física Aplicada II.

10.1021/jp904421w CCC: $40.75
Published on Web 07/06/2009

permittivity of the suspending medium, ε_0 is the vacuum permittivity, a is the particle radius, σ is the particle surface charge density, ϕ is the volume fraction of particles, and $\bar{n}_c$ and z_c are the mean number density in the liquid medium and the valence of the added counterions, respectively. Equation 1 has shown to provide unrealistic values at very low particle volume fraction and surface charge; thus a new method of estimation of κ^{-1} has been recently proposed,[21] although it requires complicated numerical computations. For more concentrated suspensions, eq 1 is a reasonable definition of the width of the EDL.

In a previous work, the equilibrium EDL of a spherical particle in a realistic aqueous salt-free concentrated suspension was studied in detail.[11] It was concluded that water dissociation ions and those coming from CO_2 contamination were determinant for modeling a real salt-free electric double layer. Even in the case of no CO_2 contamination, it was demonstrated that the H^+ and OH^- ions from water dissociation should always be taken into account because they will be unavoidably present in the solution accompanying the added counterions released by the particles. Very recently, we have explored the effects of water dissociation and CO_2 contamination on the electrophoretic mobility of a spherical particle in a salt-free concentrated suspension.[21] The results have shown the importance of the latter corrections, quite tremendous in many of the cases analyzed, in particular, but not only, for samples in contact with the atmosphere. Therefore, a revision of standard salt-free models turns out to be mandatory. The increasing numerical and computational problems associated with the above-mentioned corrections in the integro-differential Poisson−Boltzmann equation, coupled to the "realistic" salt-free differential electrokinetic equations, are more than compensated by the magnitude of the corrections involved. Solving this problem to predict real conductivity data in salt-free suspensions is the aim of the present paper.

Thus, in this work we will study the electrical conductivity of a suspension in static electric fields (angular frequency $\omega = 0$), also called dc electrical conductivity, for the cases whose EDLs were described in refs 11 and 21, concerning (i) the presence of only added counterions, (ii) the additional inclusion of H^+ and OH^- ions from water dissociation, and (iii) the further inclusion of ions originated by atmospheric CO_2 contamination. For all these cases, we have studied the dependence of the electrical conductivity on particle charge density and volume fraction. In the following sections we describe the cell model approach used in our model and compare between theoretical dc electrical conductivity predictions of pure and realistic salt-free suspensions. As we will see, and similar to what was shown for realistic salt-free electrophoresis, the conductivity suffers enormous changes when the realistic corrections are included in the model.

Theory

The Cell Model. Due to the complex nature of real concentrated suspensions where electro-hydrodynamic interactions play a decisive role in understanding the dynamics of these systems, the use of mean-field approaches is of worth. The cell models can help us in representing the average hydrodynamic interactions between a representative particle and its neighboring medium in addition to the overlapping of adjacent electric double layers. The cell model concept has been successfully applied to the study of the electrokinetics and rheology of concentrated suspensions. Phenomena such as static electrophoresis and electrical conductivity,[22−25] sedimentation velocity and potential,[26,27] dynamic electrophoresis,[12,28−30] complex conductivity and dielectric response,[13,31] electroviscous effect,[32−34] and electroacoustic phenomena,[35,36] have been addressed in terms of cells. An excellent review on the use of the spherical cell model has been recently written by Zholkovskij et al.[37]

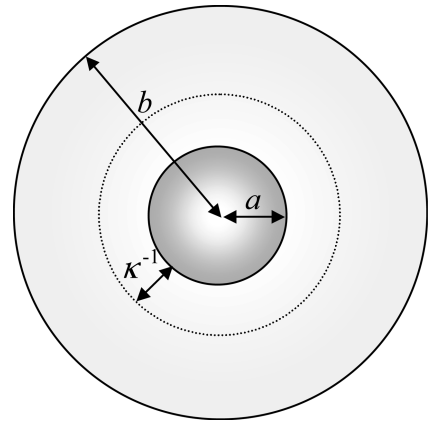

Figure 1. The cell model.

According to this model (Figure 1), each spherical particle of radius a is surrounded by a concentric shell of the liquid medium, having an outer radius b such that the particle/cell volume ratio in the cell is equal to the particle volume fraction throughout the entire suspension,[38,39] i.e.

$$\phi = \left(\frac{a}{b}\right)^3 \tag{2}$$

The basic assumption of the cell model is that the suspension properties can be derived from the study of a unique cell for homogeneous and isotropic suspensions.

Electrokinetic Equations and Boundary Conditions. Let us consider a charged spherical particle with surface charge density σ, which is immersed in an aqueous solution of relative permittivity ε_{rs} and viscosity η_s, that contains added counterions of valence z_c and drag coefficient λ_c, which stem from the charge generation process on the particles, as well as others, for the moment, unspecified ionic species. We will henceforth represent the ionic species with an index j ($j = 1,..., n$), with valence z_j and drag coefficient λ_j, being the added counterion species associated with the value $j = 1$, i.e., $z_1 = z_c$ and $\lambda_1 = \lambda_c$. The axes of a spherical coordinate system (r, θ, φ) are fixed at the center of the particle, with the polar axis ($\theta = 0$) parallel to the static electric field $\mathbf{E}$. We need to know the electrical potential $\Psi(\mathbf{r})$, the number density of ions $n_j(\mathbf{r})$ ($j = 1,..., n$), their drift velocity $\mathbf{v}_j(\mathbf{r})$ ($j = 1,..., n$), the fluid velocity $\mathbf{v}(\mathbf{r})$, and the pressure $p(\mathbf{r})$. The fundamental equations connecting them are well-known:[28,40−42]

$$\nabla^2\Psi(\mathbf{r}) = -\frac{\rho_{el}(\mathbf{r})}{\varepsilon_{rs}\varepsilon_0} \tag{3}$$

$$\rho_{el}(\mathbf{r}) = \sum_{j=1}^{n} z_j e n_j(\mathbf{r}) \tag{4}$$

$$\eta_s\nabla^2\mathbf{v}(\mathbf{r}) - \nabla p(\mathbf{r}) - \rho_{el}(\mathbf{r})\,\nabla\Psi(\mathbf{r}) = 0 \tag{5}$$

$$\nabla \cdot \mathbf{v}(\mathbf{r}) = 0 \tag{6}$$

$$\mathbf{v}_j(\mathbf{r}) = \mathbf{v}(\mathbf{r}) - \frac{1}{\lambda_j}\nabla\mu_j(\mathbf{r}) \quad (j = 1, ..., n) \tag{7}$$

$$\mu_j(\mathbf{r}) = \mu_j^{\infty} + z_j e\Psi(\mathbf{r}) + k_B T \ln n_j(\mathbf{r}) \quad (j = 1, ..., n) \tag{8}$$

$$\nabla \cdot \left[\sum_{j=1}^{N} z_j e n_j(\mathbf{r})\, \mathbf{v}_j(\mathbf{r})\right] = 0 \tag{9}$$

$$\nabla \cdot [n_c(\mathbf{r})\, \mathbf{v}_c(\mathbf{r})] = 0 \tag{9'}$$

where $\mu_j(\mathbf{r})$ is the electrochemical potential of the jth ionic species, with μ_j^{∞} its standard value. Equation 3 is Poisson's equation, where $\rho_{el}(\mathbf{r})$ is the electric charge density given by eq 4. Equations 5 and 6 are the Navier−Stokes equations appropriate to a steady incompressible fluid flow at low Reynolds number in the presence of an electrical body force. Equation 7 means that the ionic flow is provoked by the liquid flow and the gradient of the electrochemical potential defined in eq 8, and it is related to the Nernst−Planck equations for ionic fluxes. The drag coefficient λ_j in eq 7 is related to the limiting ionic conductance Λ_j^0 by[40]

$$\lambda_j = \frac{N_A e^2 |z_j|}{\Lambda_j^0} \quad (j = 1, ..., n) \tag{10}$$

where N_A is Avogadro's number. The continuity eq 9 stands for charge conservation instead of conservation of the number of every ionic species in the system. Besides, we assume that the possible chemical reactions that take place in the system are faster than any other ionic processes in response to the applied constant electric field, to ensure chemical local equilibrium in every point of the suspensions. To completely solve the problem, we need additional equations that can be obtained from the equilibrium scheme for chemical reactions. Thus, their mass-action equations will be used locally in addition to the latter general system of equations 3−9. For the case the added counterions were of a different ionic species from those associated with water dissociation and CO_2 contamination, its concentration will not be linked with the other ones by chemical reactions. Therefore, a continuity equation for the conservation of the number of just the added counterions (eq 9′), in addition to the general continuity equation for the charge conservation (eq 9), will be used. The boundary conditions of the electrokinetic equations under the cell model approximation have been extensively dealt with.[28,9] Briefly, they are the null net force acting on the particle or the unit cell, the continuity of the electrical potential and the discontinuity of the normal component of the electrical displacement at the particle surface, the nonslip condition for the liquid on the particle surface, the impenetrability of ions through the particle surface, the null vorticity of the liquid flow at the outer surface of the cell, and others of the Shilov−Zharkikh−Borkovskaya model.[43]

The equilibrium volume charge density is given by

$$\rho_{el}^{(0)}(r) = \sum_{j=1}^{n} z_j e n_j^{(0)}(r) \tag{11}$$

and the equilibrium ionic concentrations

$$n_j^{(0)}(r) = b_j \exp\left(-\frac{z_j e\Psi^{(0)}(r)}{k_B T}\right) \quad (j = 1, ..., n) \tag{12}$$

obey the Boltzmann distribution. The unknown prefactors b_j ($j = 1,..., n$) represent the concentration of ions at a point where the electrical potential is set to zero, which for numerical convenience is chosen at the outer surface of the cell:

$$\Psi^{(0)}(b) = 0 \tag{13}$$

For the case of just one ionic species, the added counterions ($j = 1$ case), electroneutrality leads to the condition

$$\int_a^b [n_c^{(0)}(r)](4\pi r^2)\, dr = \int_a^b b_c \exp\left(-\frac{z_c e\Psi^{(0)}(r)}{k_B T}\right)(4\pi r^2)\, dr = \frac{-4\pi a^2\sigma}{z_c e} \tag{14}$$

The Poisson−Boltzmann equation

$$\frac{1}{r^2}\frac{d}{dr}\left(r^2 \frac{d\Psi^{(0)}}{dr}\right) = -\frac{1}{\varepsilon_{rs}\varepsilon_0} z_c e n_c^{(0)}(r) \tag{15}$$

becomes integro-differential with

$$n_c^{(0)}(r) = \frac{(-4\pi a^2\sigma)\exp\left(-\frac{z_c e\Psi^{(0)}(r)}{k_B T}\right)}{z_c e\int_a^b \exp\left(-\frac{z_c e\Psi^{(0)}(r)}{k_B T}\right)(4\pi r^2)\, dr} \tag{16}$$

and its boundary conditions is expressed by eq 14 and

$$\frac{d\Psi^{(0)}}{dr}(b) = 0 \tag{17}$$

or, alternatively, by eq 17 and

$$\frac{d\Psi^{(0)}}{dr}(a) = -\frac{\sigma}{\varepsilon_{rs}\varepsilon_0} \tag{18}$$

coming from the electroneutrality of the cell and Gauss theorem. Whether the added counterions are coincident or not with one of the other ionic species in the system can give rise to important changes in conductivity predictions. Those cases will be properly analyzed in further sections.

We are concerned here with the linear response of the suspension to the (low strength) applied electric field, so a perturbation scheme where the perturbation quantities are linearly dependent on the field will be followed. For a detailed description of boundary conditions in terms of perturbation quantities, the reader is encouraged to see earlier papers where complete studies can be found.[3,9,25,29,30,44] We use the mathematical application MATLAB with its built-in routines to numerically solve the latter linear set of differential equations.

Previously, we had to solve the equilibrium Poisson−Boltzmann equation coupled with the equations for the ionic equilibrium chemical reactions to obtain the unknown concentration prefactors b_j ($j = 1,..., n$). The boundary value problem solver used is a finite difference code that implements the three-stage Lobatto−Illa formula. This is a collocation formula and the collocation polynomial provides a C^1-continuous solution that is fourth order accurate uniformly in the function domain.[45] Mesh selection and error control are based on the residual of the continuous solution. The relative tolerance, which applies to all components of the residual vector, has been taken equal to 10^{-6}.

Electrical Conductivity. The electrical conductivity, K, of the suspension, is usually defined in terms of the volume averages of the local electric current density and electric field in a cell representing the whole suspension

$$\langle \mathbf{i} \rangle = \frac{1}{V_{\text{cell}}} \int_{V_{\text{cell}}} \mathbf{i}(\mathbf{r})\, \mathrm{d}V = K \langle \mathbf{E} \rangle \tag{19}$$

The macroscopic electric field $\langle \mathbf{E} \rangle$ is given by

$$\langle \mathbf{E} \rangle = -\frac{1}{V_{\text{cell}}} \int_{V_{\text{cell}}} \nabla \Psi(\mathbf{r})\, \mathrm{d}V \tag{20}$$

The electric current density of a suspension is defined by

$$\mathbf{i}(\mathbf{r}) = \sum_{j=1}^{n} z_j e n_j(\mathbf{r})\, \mathbf{v}_j(\mathbf{r})$$

$$= \sum_{j=1}^{n} z_j e n_j(\mathbf{r}) [\mathbf{v}(\mathbf{r}) - \nabla \mu_j(\mathbf{r})/\lambda_j] \tag{21}$$

By following a similar procedure as that described for the conductivity of suspensions in salt solutions,[44] the electrical conductivity of a concentrated suspension in a realistic salt-free medium with n ionic species is given by

$$K = \frac{b}{Y(b)} \sum_{j=1}^{n} \left\{ \frac{z_j^2 e^2}{\lambda_j} \frac{\mathrm{d}\phi_j}{\mathrm{d}r}(b) - 2\frac{h(b)}{b} z_j e \right\} b_j \exp\left(-\frac{z_j e \Psi^0(b)}{K_{\text{B}} T} \right) \tag{22}$$

The functions $\phi_j(r)$ ($j = 1,..., n$), $Y(r)$, and $h(r)$ represent the radial-dependent part of the perturbations in electrochemical potential, local electric field, and fluid velocity, respectively (see refs 4, 9, and 21, where more mathematical details are given). The coefficients b_j ($j = 1,..., n$) are derived depending on whether the added counterions are coincident or not with one of the other ionic species in the system, and according to the procedure developed from the authors in ref 11. The latter expression is obtained in the particle reference frame. If we change to the laboratory reference system where the particles move with the electrophoretic velocity $\mu\mathbf{E}$, we must change eq 21 to also account for the contribution of the charged particles. In the Appendix, it is shown that the so-obtained conductivity in the laboratory reference frame is equivalent to that according eq 21 in the moving particle reference system.

There have been different experimental approaches to conductivity yielding more or less sophisticated heuristic formulas to describe the dc conductivity of salt-free suspensions. One of the first was developed by Schaefer[46] neglecting the macro-ion contribution. A more sophisticated one was proposed by Deggelmann et al.[47] Data on the concentration dependence of highly charged latex spheres has been also reported by Hessinger et al.[48] In the past few years some conductivity models valid for pure salt-free suspensions have been developed. Ohshima derived one for low particle concentration and got analytical expressions for the electrical conductivity.[49] His main conclusions were that the electrical conductivity follows two distinct behaviors separated by a certain critical surface charge value. Because of the counterion condensation effect, for charges higher than the critical one the electrical conductivity attains a plateau and becomes poorly dependent on particle charge. The authors of the present work have also addressed the conductivity of pure salt-free suspensions in a very recent contribution where different frames of boundary conditions, typically found in the literature, were explored.[9]

In what follows we will analyze the conductivity of more "realistic" salt-free suspensions including water dissociation and water dissociation plus CO_2 contamination, comparing with pure salt-free conductivity predictions. A first and crucial step before addressing that issue is to solve the equilibrium integro-differential Poisson−Boltzmann equation for the cases we are concerned with, because the equilibrium electrical potential $\Psi^{(0)}(r)$ explicitly appears in the differential electrokinetic equations.

Realistic Corrections to the dc Electrical Conductivity: Water Dissociation and CO_2 Contamination. We now explore the effect on the conductivity of the latter two realistic situations. In the first one, we will suppose that there are also H^+ and OH^- ions coming from water dissociation in the aqueous solution in addition to the added counterions. In such a scenario we can distinguish the cases: (a) the added counterions coincide with H^+ or OH^- ions (number of different ionic species $n = 2$), and (b) they are all of a different ionic species ($n = 3$). This distinction is quite relevant because in the (a) case the added counterions will enter the reaction equation for water dissociation, whereas in the (b) case they do not. In the second realistic situation we extend the first one to also include ions stemming from the atmospheric CO_2 contamination in the liquid medium. Again, we can distinguish between two cases: (a) when the added counterions are coincident with one of the ionic species in the system (H^+, OH^-, HCO_3^- ions) ($n = 3$), thus entering in one of the equilibrium dissociation equations, and (b) when they are of a different ionic species ($n = 4$) and, therefore, not related to any equilibrium dissociation equation. For both realistic cases the water dissociation reaction

$$H_2O \rightleftarrows H^+ + OH^- \tag{23}$$

is fulfilled. For the second one the following equations will play an important role:

$$\left.\begin{aligned} CO_2 + H_2O &\rightleftarrows H_2CO_3 \\ H_2CO_3 &\rightleftarrows H^+ + HCO_3^- \end{aligned}\right\}$$
$$HCO_3^- \rightleftarrows H^+ + CO_3^{2-} \tag{24}$$

As already reported,[11] the role of CO_3^{2-} ions can be neglected because of the lower dissociation constant of their chemical dissociation reaction. The resolution of the Poisson−Boltzmann equation and its application to the electrophoresis in realistic salt-free suspensions for the above-mentioned situations can be

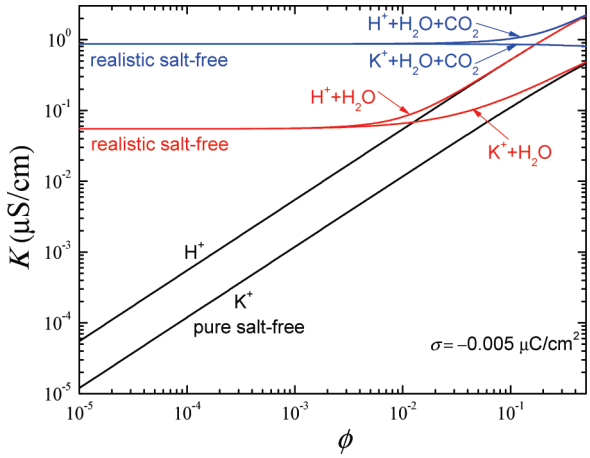

Figure 2. Electrical conductivity against particle volume fraction of pure salt-free suspensions with added counterions H^+ or K^+, realistic salt-free suspensions with added counterions H^+ or K^+ + water dissociation, and realistic salt-free suspensions with added counterions H^+ or K^+ + water dissociation + CO_2 contamination. Particle surface charge density -0.005 $\mu C/cm^2$.

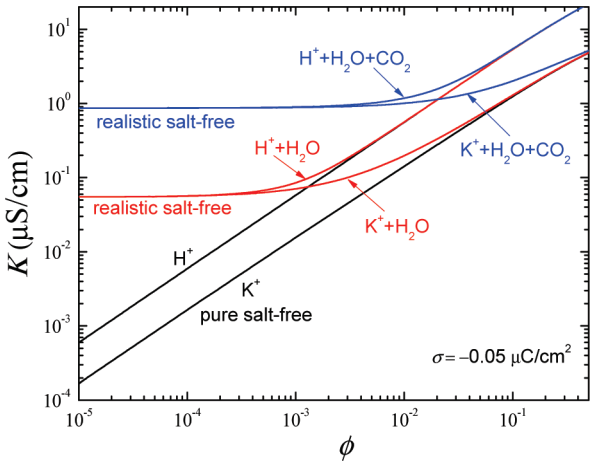

Figure 3. Same as Figure 2 but with particle surface charge density -0.05 $\mu C/cm^2$.

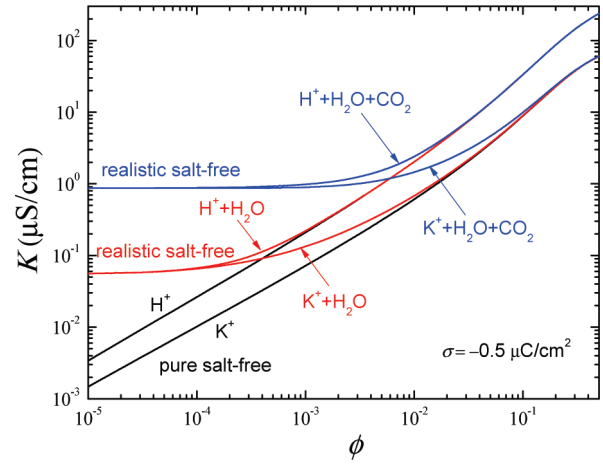

Figure 4. Same as Figure 2 but with particle surface charge density -0.5 $\mu C/cm^2$.

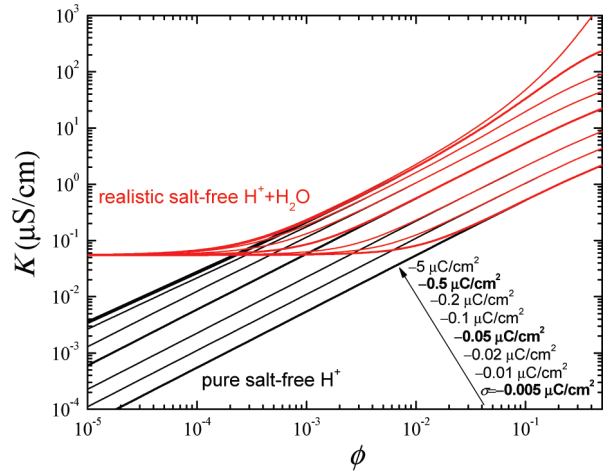

Figure 5. Electrical conductivity against particle volume fraction of pure salt-free suspensions with added counterions H^+ and realistic salt-free suspensions with added counterions H^+ + water dissociation, for different particle surface charge densities.

found in refs 11 and 21 from the authors, where a full description of the mathematical details is given.

Results and Discussion

Electrical Conductivity against Particle Volume Fraction. In Figures 2, 3, 4, 5, 6, and 7, the temperature T, the relative permittivity of the suspending liquid ε_{rs}, and the radius of the particles have been chosen as 298.16 K, 78.55, and 100 nm, respectively. In Figures 2−4 we show for different particle surface charge densities and two different added counterion species the effect of including water dissociation ions and others stemming from CO_2 contamination on the electrical conductivity of a salt-free suspension in comparison with pure salt-free cases with just the same added counterions.

First of all and regarding the conductivity−volume fraction behavior for realistic salt-free suspensions with different added counterions and water dissociation, we can conclude the following:

(i) For every particle charge, the conductivity increases with volume fraction for pure salt-free suspensions due to the increasing concentration of charged particles and added counterions in the medium per unit volume. Also, increasing particle charge at fixed volume fraction increases consequently the conductivity. Furthermore, the larger the particle charge, the larger the number of counterions released by each particle to the unit volume. For realistic suspensions there is an initial and unique conductivity plateau at low volume fractions related to the dominance in such a region of water dissociation ions, nearly constant in concentrations. The conductivity plateau value is 0.055 μS/cm, which is exactly the conductivity of pure water.

(ii) Important differences in conductivity are obtained at high volume fractions when the previously described cases a and b are compared, associated, respectively, with the participation or not of the added counterion in the water dissociation equation. Qualitatively the roles of K^+ and H^+ counterions are similar, but while the latter enters the water dissociation reaction, the former does not, which modifies considerably the final counterion and co-ion concentrations inside the cell. In case a the total numbers of counterions (H^+) and co-ions (OH^-) are both less than the total numbers of counterions ($H^+ + K^+$) and co-ions (OH^-) of case b. In each case the net ionic charge is equal to minus the particle charge. However, in spite of the larger concentration of counterions and co-ions in case b, the conductivity is larger for case a due to the larger diffusion

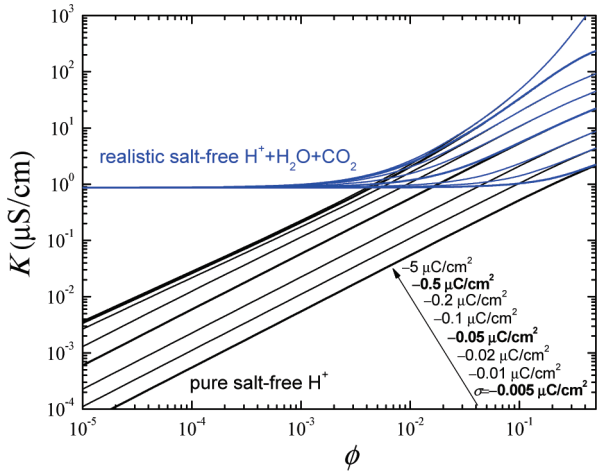

Figure 6. Electrical conductivity against particle volume fraction of pure salt-free suspensions with added counterions H^+ and realistic salt-free suspensions with added counterions H^+ + water dissociation + CO_2 contamination, for different particle surface charge densities.

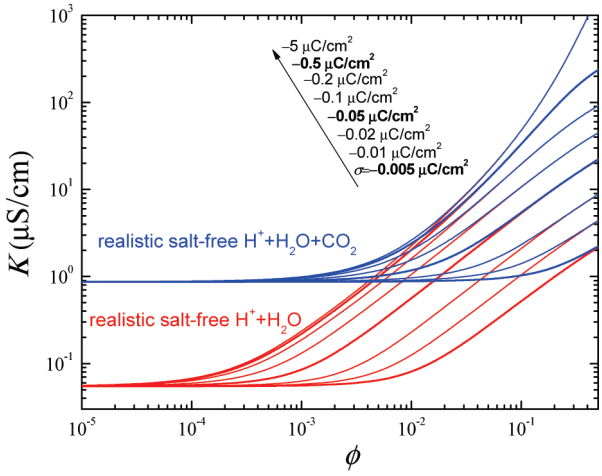

Figure 7. Electrical conductivity against particle volume fraction of realistic salt-free suspensions with added counterions H^+ + water dissociation and realistic salt-free suspensions with added counterions H^+ + water dissociation + CO_2 contamination, for different particle surface charge densities.

coefficient of H^+ ions than that of K^+ ions (around 5 times larger), and the larger concentration of the H^+ counterions in case a than in case b.

(iii) For highly concentrated suspensions there are no differences between curves corresponding to the pure suspensions (with H^+ or K^+ as added counterions) and their corresponding realistic salt-free suspensions. In this region the added counterions H^+ or K^+ stemming from the particle charging mechanism dominate those associated with water dissociation (H^+ and OH^-).

(iv) For low concentration suspensions there are no differences between curves corresponding to realistic salt-free suspensions with H^+ or K^+ as added counterions once water dissociation is taken into account. As mentioned before, at such low volume fractions water dissociation ions always dominate those from the charging process, whatever case a or b we choose.

As to the conductivity dependence on volume fraction of realistic salt-free suspensions with different added counterions, water dissociation, and CO_2 contamination, also depicted in Figures 2−4, we can draw the following conclusions:

(i) For the latter realistic suspensions there is again an initial and unique conductivity plateau at low volume fractions related to the dominance in such a region of water dissociation ions and those stemming from the dissociation of carbonic acid generated by the dissolved CO_2 in the aqueous solution, nearly constant in concentrations. The conductivity plateau value is around 0.9 μS/cm, which is the conductivity of ordinary distilled water in equilibrium with atmospheric CO_2.[50]

(ii) Important differences in conductivity are obtained at high volume fractions when the corresponding cases a and b are compared, associated, respectively, with the participation or not of the added counterion in water and carbonic acid dissociation equations. While H^+ counterions enter the latter dissociation equations, K^+ counterions do not, which again modifies considerably the final counterion and co-ion concentrations inside the cell. In case a the total numbers of counterions (H^+) and co-ions (OH^- and HCO_3^-) are both less than the total numbers of counterions (H^+ + K^+) and co-ions (OH^- and HCO_3^-) of case b. The larger diffusion coefficient of H^+ ions than that of K^+ ions and the larger concentration of counterions H^+ in case a than in case b justify once more the higher conductivity obtained for case a, in spite of the larger concentrations of total counterions and co-ions in case b.

(iii) For highly concentrated suspensions there are no differences among curves corresponding to the pure salt-free (with H^+ or K^+ as added counterions), the realistic salt-free with water dissociation, and the realistic salt-free suspensions with the additional inclusion of CO_2 contamination. In this region the added counterions H^+ or K^+ stemming from the particle charging mechanism dominate those associated with water dissociation (H^+ and OH^-) and CO_2 contamination (H^+ and HCO_3^-).

(iv) For low concentration suspensions there are no differences between curves corresponding to realistic salt-free suspensions with H^+ or K^+ as added counterions once water dissociation plus CO_2 contamination is accounted for. As mentioned before, at such low volume fractions water dissociation and CO_2 contamination ions clearly dominate the added counterions released by the particles for case a or b.

(v) The ϕ value at which the conductivity of realistic suspensions coincides with that of the pure salt-free one is larger if there is CO_2 contamination. A larger volume fraction and, consequently, a larger concentration of added counterions is necessary to overcome the effects of CO_2 contamination plus water dissociation in comparison with that of water dissociation alone, because of the larger ionic strength in atmospheric contaminated samples.

In Figure 4, for the largest charge analyzed, we can see an enhancement in conductivity over the linear increase in the log−log plot at high particle concentrations. This fact is probably due to the faster growth in added counterion concentration with the increase in volume fraction at fixed and large surface charge density. The average counterion concentration is[9] proportional to $\phi/(1-\phi)$; therefore, as the particle volume fraction increases the average counterion concentration rises largely over the linear behavior. Remember that in such a region of particle concentrations only the added counterions are important; the other effects related to water dissociation and CO_2 contamination are totally screened by the added counterions.

In Figure 5, we display the conductivity of pure (added counterions H^+) and realistic salt-free suspensions (added counterions H^+ + water dissociation) as a function of volume fraction for different particle charge densities. We extend the

particle charge region in Figure 5 to better show what was already pointed out in previous figures.

The most remarkable features associated with the inclusion of water dissociation over pure salt-free conditions are, first, the presence of a unique plateau for all particle charges if the volume fraction is sufficiently low and, second, the matching of the conductivity of realistic salt-free suspensions with their corresponding pure salt-free ones at high volume fractions. Particularly important is the large separation (orders of magnitude) between pure and realistic salt-free conductivity predictions for low volume fractions at every particle charge. This fact has tremendous consequences when it comes to comparison with salt-free experiments. Even with the most perfect experimental setup and assuring no contamination at all in the samples, if the salt-free suspension is aqueous, the theoretical prediction of the standard pure salt-free model is quite small for the latter conditions. Thus, the corrections to the standard model addressed in this paper turn out to be mandatory, even more if the samples have been also exposed to the atmosphere. This case is shown in Figure 6, where a comparison similar to that in Figure 5 is carried out, but including the effect of CO_2 contamination. Apart from the expected increase in conductivity due to the presence of additional ionic species generated by the dissolved CO_2, the plateau region now extends to larger volume fractions for every particle charge. The quantitative effect at low volume fractions is tremendous. Salt-free conductivity measurements require an extra control to guarantee that a perfectly sealed setup is maintained along the full measurement procedure, and that the samples are adequately prepared to ensure they are free from parasitic CO_2 and subsequent generated species in aqueous solution.

To clearly show the effects of water dissociation and water dissociation plus CO_2 contamination on the conductivity of salt-free suspensions, in Figure 7 we represent just the realistic salt-free cases of previous figures. The idea is to underline the influence of parasitic atmospheric contamination over what we can consider the conductivity of a perfect real salt-free aqueous suspension: ultrapure water + added counterions (H^+ in this study). With the exception of the region of moderate−large concentrated suspensions (depending on the charge), the conductivity can be an order of magnitude larger in contaminated samples, or even more, which reflects the importance of the purity of the samples when working with salt-free suspensions.

Electrical Conductivity: Field-Induced Current Density Contributions. We can go a step further by exploring the field-induced electric current density around a particle inside a cell, which is composed by electromigrative $\vec{\mathbf{J}}_e(\vec{\mathbf{r}})$, diffusive $\vec{\mathbf{J}}_d(\vec{\mathbf{r}})$, and conductive $\vec{\mathbf{J}}_c(\vec{\mathbf{r}})$ contributions, for pure and realistic salt-free suspensions. For brevity, we will only analyze the cases "a" described in previous sections where the added counterions coincide with one of the other ionic species stemming from water dissociation or CO_2 contamination. The radial and θ components of the field-induced electric current density contributions can be expressed as

$$\vec{\mathbf{J}}_e(\vec{\mathbf{r}})\cdot\hat{\mathbf{r}} = \left[\frac{z_{H^+}{}^2 e^2 n^0_{H^+}(r)}{\lambda_{H^+}} + \frac{z_{OH^-}{}^2 e^2 n^0_{OH^-}(r)}{\lambda_{OH^-}} + \frac{z_{HCO_3^-}{}^2 e^2 n^0_{HCO_3^-}(r)}{\lambda_{HCO_3^-}}\right]\frac{dY}{dr} E\cos\theta \quad (25)$$

$$\vec{\mathbf{J}}_e(\vec{\mathbf{r}})\cdot\hat{\boldsymbol{\theta}} = -\left[\frac{z_{H^+}{}^2 e^2 n^0_{H^+}(r)}{\lambda_{H^+}} + \frac{z_{OH^-}{}^2 e^2 n^0_{OH^-}(r)}{\lambda_{OH^-}} + \frac{z_{HCO_3^-}{}^2 e^2 n_{HCO_3^-}{}^0(r)}{\lambda_{HCO_3^-}}\right]\frac{Y(r)}{r} E\sin\theta \quad (26)$$

$$\vec{\mathbf{J}}_d(\vec{\mathbf{r}})\cdot\hat{\mathbf{r}} = \left[\frac{z_{H^+}{}^2 e^2 n^0_{H^+}(r)}{\lambda_{H^+}}\left(\frac{d\phi_{H^+}}{dr} - \frac{dY}{dr}\right) + \frac{z_{OH^-}{}^2 e^2 n^0_{OH^-}(r)}{\lambda_{OH^-}}\left(\frac{d\phi_{OH^-}}{dr} - \frac{dY}{dr}\right) + \frac{z_{HCO_3^-}{}^2 e^2 n^0_{HCO_3^-}(r)}{\lambda_{HCO_3^-}}\left(\frac{d\phi_{HCO_3^-}}{dr} - \frac{dY}{dr}\right)\right] E\cos\theta \quad (27)$$

$$\vec{\mathbf{J}}_d(\vec{\mathbf{r}})\cdot\hat{\boldsymbol{\theta}} = \left[\frac{z_{H^+}{}^2 e^2 n^0_{H^+}(r)}{\lambda_{H^+}}\left(-\frac{\phi_{H^+}}{r} + \frac{Y}{r}\right) + \frac{z_{OH^-}{}^2 e^2 n^0_{OH^-}(r)}{\lambda_{OH^-}}\left(-\frac{\phi_{OH^-}}{r} + \frac{Y}{r}\right) + \frac{z_{HCO_3^-}{}^2 e^2 n^0_{HCO_3^-}(r)}{\lambda_{HCO_3^-}}\left(-\frac{\phi_{HCO_3^-}}{r} + \frac{Y}{r}\right)\right] E\sin\theta \quad (28)$$

$$\vec{\mathbf{J}}_c(\vec{\mathbf{r}})\cdot\hat{\mathbf{r}} = -\left[z_{H^+} e n^0_{H^+}(r) + z_{OH^-} e n^0_{OH^-}(r) + z_{HCO_3^-} e n^0_{HCO_3^-}(r)\right]\left(\frac{2h}{r}\right) E\cos\theta \quad (29)$$

$$\vec{\mathbf{J}}_c(\vec{\mathbf{r}})\cdot\hat{\boldsymbol{\theta}} = \left[z_{H^+} e n^0_{H^+}(r) + z_{OH^-} e n^0_{OH^-}(r) + z_{HCO_3^-} e n^0_{HCO_3^-}(r)\right]\left(\frac{h}{r} + \frac{dh}{dr}\right) E\sin\theta \quad (30)$$

for the general case of added counterions + water dissociation + CO_2 contamination. When the pure salt-free case is concerned, the latter equations are still valid if one neglects in every equation the ionic terms different from that associated with the added counterions. Analogously, for the case of added counterion + water dissociation, the terms related to the HCO_3^- ion must be deleted. In the next figures, we display nondimensional field-induced current density contributions obtained by dividing the first member of the latter equations by the scaling factor

$$\frac{(\varepsilon_{rs}\varepsilon_0 k_B T)^2}{\eta_s a^2 e^2} E \quad (31)$$

We have chosen for the study in Figures 8, 9, and 10 the theoretical conditions $\phi = 0.0001$ and $\sigma = -0.005$ μC/cm^2, where important deviations between realistic and pure salt-free electrical conductivities have been predicted (see Figures 5−7). Thus, we show in Figure 8 the pure salt-free case, in Figure 9 the realistic one with water dissociation, and in Figure 10 that with water dissociation and CO_2 contamination. In each figure we display in the upper panels the vector fields of the three electrical contributions to the field-induced current density in a region close to the particle. In the bottom panels of the same

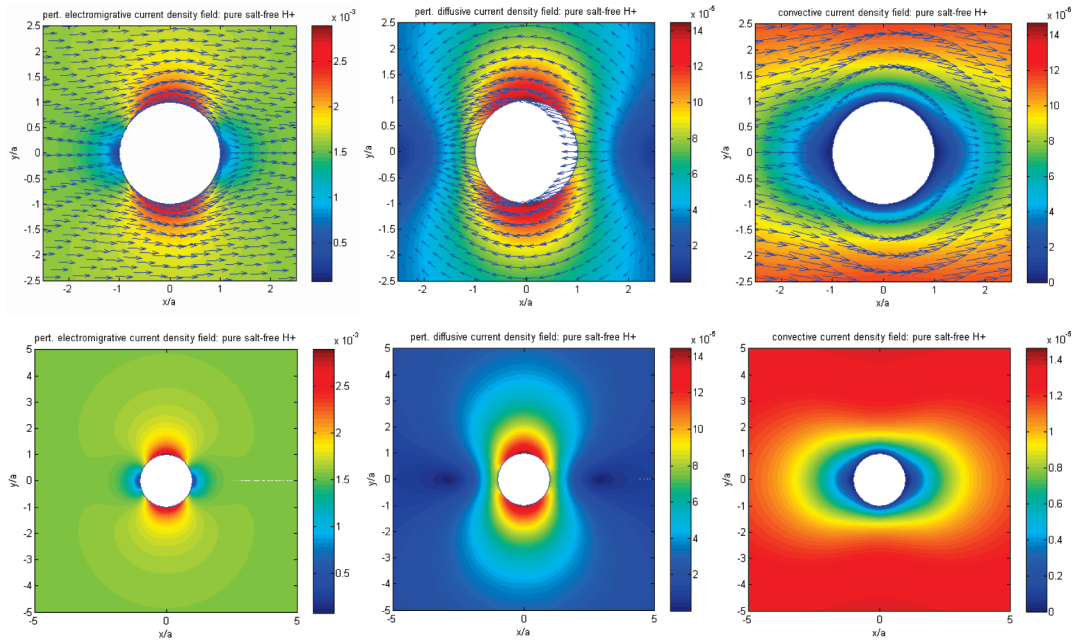

Figure 8. Two-dimensional plots of nondimensional field-induced current density contributions in a pure salt-free suspension at 25 °C with H^+ as added counterions. $a = 100$ nm, $\phi = 0.0001$, and $\sigma = -0.005$ μC/cm^2. In the figures the electric field points to the right.

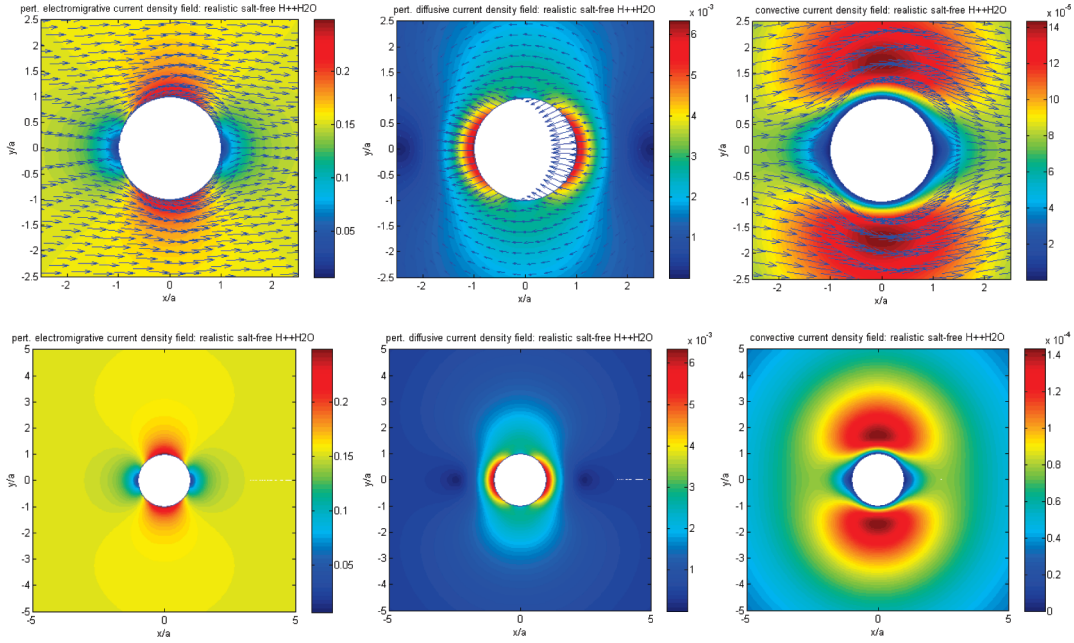

Figure 9. Two-dimensional plots of nondimensional field-induced current density contributions in a realistic salt-free suspension at 25 °C with H^+ as added counterions + water dissociation. $a = 100$ nm, $\phi = 0.0001$, and $\sigma = -0.005$ μC/cm^2. In the figures the electric field points to the right.

figure we extend the latter region to clearly show the changes that take place in current density as we move further from the particle surface. For clarity of the graphs in the bottom panels, we represent the modulus of the vectors corresponding to the current density contributions. The general vector pattern can be observed in the upper panels.

While the electromigrative contributions are qualitatively similar for pure and realistic salt-free cases, important changes can be found when convective and mainly diffusive patterns of pure and realistic salt-free suspensions are compared. The most important diffusion regions migrate from a direction perpendicular to the electric field (pure salt-free case) to that of the polar axis (direction of the electric field) (realistic cases). This fact is associated with the change in perturbed ionic concentrations at both sides of the particles due to the electric field as ionic strength increases from pure to realistic salt-free cases.[21]

On the other hand, it is the electromigrative contribution that is the most important from the quantitative point of view in all cases studied, followed by the net diffusive contribution. The electric polarization of the double layer greatly influences the final electrokinetic behavior of the system. In the stationary cases studied in Figures 8−10, tangential counterion fluxes from the left to the right parts of the particles (the opposite for co-ions) are mainly responsible for the magnitude of induced charges. When co-ions are present, their role is comparatively smaller than that of counterions. These contributions generate a net dipole moment pointing in the direction of the electric field. Simultaneously, diffusion currents tend to diminish the ac-

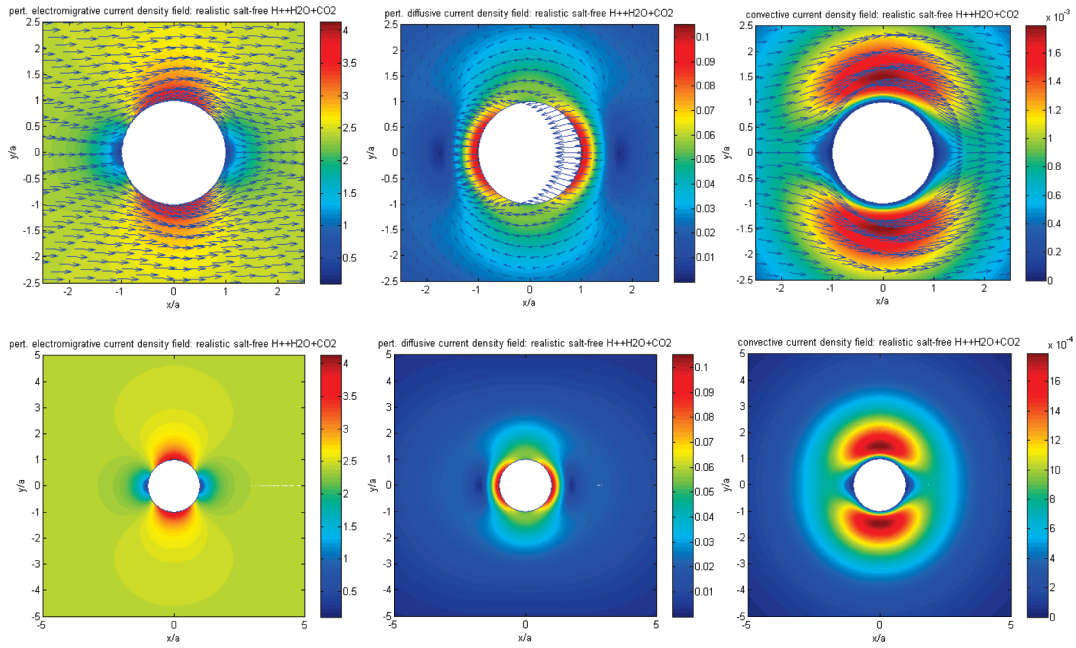

Figure 10. Two-dimensional plots of nondimensional field-induced current density contributions in a realistic salt-free suspension at 25 °C with H^+ as added counterions + water dissociation + CO_2 contamination. $a = 100$ nm, $\phi = 0.0001$, and $\sigma = -0.005$ μC/cm^2. In the figures the electric field points to the right.

cumulation (depletion) of ions at both sides of the particle provoked by the field, decreasing the magnitude of the induced dipole moment until the stationary state is attained. These net diffusion currents from the right to the left parts of the particles are clearly displayed in Figures 8−10, being more important as more ionic species participate (the realistic salt-free case with water dissociation plus CO_2 contamination) for the same added counterions H^+.

Likewise, the convective contributions are increasingly important as ionic strength increases from pure to realistic salt-free suspensions in the region close to the particles. The expected compression of the EDLs upon increasing ionic strength seems to confine the convective effects to distances closer to the particles, where the non-electroneutrality prevails.

Conclusions

Based on a "realistic" description of the electric double layer for salt-free concentrated suspensions[11] which incorporates effects as water dissociation and CO_2 contamination in the suspensions, we have studied how these effects modify the dc electrical conductivity of a salt-free suspension. The numerical results have shown the importance of the latter realistic effects in most typical conditions. The enhancement in conductivity is larger the lower the volume fraction, but is still more relevant if in addition to water dissociation we allow for atmospheric CO_2 contamination. The results also show that it is important to distinguish whether the added counterions coincide or not with one of the ionic species arising from the dissociation of water and carbonic acid. New conductivity experiments with both clean and contaminated salt-free samples after exposure to the atmosphere could help us quantitatively check the predictions of the extended model. In any case and whatever the parameters chosen for particles and ions in solution, the inclusion of water dissociation effects has to be imperative when it comes to aqueous salt-free suspensions. The correction for CO_2 contamination clearly indicates what might be expected in conductivity from the quantitative point of view, if salt-free suspensions are allowed to be in contact with the atmosphere during their preparation or along the measurement process. We think that the present work establishes the starting point for the development of future theories concerning, particularly, the dynamic electrophoresis and dielectric response of such systems.

Acknowledgment. Financial support for this work by Ministerio de Educación y Ciencia, Spain, Project FIS2007-62737, and Junta de Andalucía, Spain, Project P08-FQM-03779, cofinanced with FEDER funds by the EU, is gratefully acknowledged.

Appendix: Electrical Conductivity and Reference Systems

Let $\mathbf{r}'_p$ be the position of the moving particle in a constant electric field $\mathbf{E}$, $\mu\mathbf{E}$ its velocity, and $\mathbf{r}'$ the position vector, in the laboratory reference system (LRS). The position vector in the particle reference system (PRS) is $\mathbf{r} = \mathbf{r}' - \mathbf{r}'_p$. The velocity in the PRS is $\mathbf{v} = \mathbf{v}' - \mathbf{v}'_p = \mathbf{v}' - \mu\mathbf{E}$ ($\mu\mathbf{E}$ is also the velocity of the PRS in the LRS). The average current density in the LRS is calculated as

$$\langle \mathbf{i}' \rangle_{LRS} = \frac{1}{V_{susp}} \int_{V_{susp}} \mathbf{i}'\, dV = \frac{1}{N_{cells} V_{cell}} \sum_{i=1}^{N_{cells}} \int_{V_{cell}} \mathbf{i}'\, dV = \frac{1}{N_{cells} V_{cell}} N_{cells} \int_{V_{cell}} \mathbf{i}'\, dV = \frac{1}{V_{cell}} \int_{V_{cell}} \mathbf{i}'\, dV$$

The current density in the LRS system inside a single cell is

$$\mathbf{i}'(\mathbf{r}') = \rho_p \mathbf{v}'_p + \sum_{j=1}^{n} \rho_j \mathbf{v}'_j = Q_p \delta(\mathbf{r}' - \mathbf{r}'_p)\mu\mathbf{E} + \sum_{j=1}^{n} [\rho_j \mathbf{v}'_j](\mathbf{r}')$$

where Q_p, ρ_j, and $\mathbf{v}'_j$ are the particle charge (only one per cell), the ion charge density, and the velocity of the j-ionic species

($j = 1,..., n$), respectively. In the PRS the current density is $\mathbf{i}(\mathbf{r}) = \sum_{j=1}^{n} [\rho_j \mathbf{v}_j](\mathbf{r})$, where $\mathbf{v}_j$ is the velocity of the j-ionic species in the PRS: $\mathbf{v}_j = \mathbf{v'}_j - \mu\mathbf{E}$. Then

$$\langle \mathbf{i'} \rangle_{\mathrm{LRS}} = \frac{1}{V_{\mathrm{cell}}} \int_{V_{\mathrm{cell}}} \mathbf{i'}\, \mathrm{d}V = \frac{1}{V_{\mathrm{cell}}} \int_{V_{\mathrm{cell}}} Q_{\mathrm{p}} \delta(\mathbf{r'} - \mathbf{r'}_{\mathrm{p}}) \mu\mathbf{E}\, \mathrm{d}V +$$

$$\frac{1}{V_{\mathrm{cell}}} \sum_{j=1}^{n} \int_{V_{\mathrm{cell}}} \rho_j \mathbf{v'}_j\, \mathrm{d}V = \frac{1}{V_{\mathrm{cell}}} Q_{\mathrm{p}} \mu\mathbf{E} +$$

$$\frac{1}{V_{\mathrm{cell}}} \sum_{j=1}^{n} \int_{V_{\mathrm{cell}}} \rho_j (\mathbf{v}_j + \mu\mathbf{E})\, \mathrm{d}V = \frac{1}{V_{\mathrm{cell}}} Q_{\mathrm{p}} \mu\mathbf{E} +$$

$$\frac{1}{V_{\mathrm{cell}}} \mu\mathbf{E} \sum_{i=1}^{n} \int_{V_{\mathrm{cell}}} \rho_j\, \mathrm{d}V + \frac{1}{V_{\mathrm{cell}}} \sum_{j=1}^{n} \int_{V_{\mathrm{cell}}} \rho_j \mathbf{v}_j\, \mathrm{d}V =$$

$$\frac{1}{V_{\mathrm{cell}}} Q_{\mathrm{p}} \mu\mathbf{E} + \frac{1}{V_{\mathrm{cell}}} \mu\mathbf{E}(-Q_{\mathrm{p}}) + \frac{1}{V_{\mathrm{cell}}} \sum_{j=1}^{n} \int_{V_{\mathrm{cell}}} \rho_j \mathbf{v}_j\, \mathrm{d}V =$$

$$\frac{1}{V_{\mathrm{cell}}} \int_{V_{\mathrm{cell}}} \mathbf{i}\, \mathrm{d}V = \langle \mathbf{i} \rangle_{\mathrm{PRS}}$$

which coincides with eq 19. In attaining the latter result, the Dirac-delta displacement property $\int_{V_{\mathrm{cell}}} \delta(\mathbf{r'} - \mathbf{r'}_{\mathrm{p}})\, \mathrm{d}\mathbf{V} = 1$ and the electroneutrality of the cell $\sum_{j=1}^{n} \int_{V_{\mathrm{cell}}} \rho_j\, \mathrm{d}V = -Q_{\mathrm{p}}$ have been used. Therefore, the conductivity can be calculated according to eq 19 in a particle reference system that moves parallel to the constant electric field.

References and Notes

(1) Medebach, M.; Palberg, T. *J. Chem. Phys.* **2003**, *119*, 3360.
(2) Medebach, M.; Palberg, T. *Colloids Surf., A* **2003**, *222*, 175.
(3) Chiang, C. P.; Lee, E.; He, Y. Y.; Hsu, J. P. *J. Phys. Chem. B* **2006**, *110*, 1490.
(4) Ohshima, H. *J. Colloid Interface Sci.* **2002**, *247*, 18.
(5) Ohshima, H. *J. Colloid Interface Sci.* **2002**, *248*, 499.
(6) Ohshima, H. *J. Colloid Interface Sci.* **2003**, *262*, 294.
(7) Ohshima, H. *J. Colloid Interface Sci.* **2003**, *265*, 422.
(8) Ruiz-Reina, E.; Carrique, F. *J. Phys. Chem. C* **2007**, *111*, 141.
(9) Carrique, F.; Ruiz-Reina, E.; Arroyo, F. J.; Delgado, A. V. *J. Phys. Chem. B* **2006**, *110*, 18313.
(10) Ohshima, H. *Theory of Colloid and Interfacial Electric Phenomena*; Academic Press: Amsterdam, The Netherlands, 2006.
(11) Ruiz-Reina, E.; Carrique, F. *J. Phys. Chem. B* **2008**, *112*, 11960.
(12) Carrique, F.; Ruiz-Reina, E.; Arroyo, F. J.; Jimenez, M. L.; Delgado, A. V. *Langmuir* **2008**, *24*, 2395.
(13) Carrique, F.; Ruiz-Reina, E.; Arroyo, F. J.; Jimenez, M. L.; Delgado, A. V. *Langmuir* **2008**, *24*, 11544.
(14) Alexander, S. *J. Chem. Phys.* **1984**, *80*, 5776.
(15) Robbins, M. O.; Kremer, K.; Grest, G. S. *J. Chem. Phys.* **1988**, *88*, 3286.
(16) Palberg, T.; Monch, W.; Bitzer, F.; Leiderer, P.; Belloni, L.; Bellini, T.; Piazza, R. *Helv. Phys. Acta* **1994**, *67*, 225.
(17) Belloni, L. *Colloids Surf., A* **1998**, *140*, 227.
(18) Levin, Y. *Rep. Prog. Phys.* **2002**, *65*, 1577.
(19) Bucci, S.; Fagotti, C.; Degiorgio, V.; Piazza, R. *Langmuir* **1991**, *7*, 824.
(20) Russel, W. B.; Saville, D. A.; Schowalter, W. R. *Colloidal Dispersions*; Cambrige University Press: Cambridge, U.K., 1989.
(21) Carrique, F.; Ruiz-Reina, E. *J. Phys. Chem. B* **2009**, *113*, 8613.
(22) Levine, S.; Neale, G. H. *J. Colloid Interface Sci.* **1974**, *47*, 520.
(23) Ohshima, H. *J. Colloid Interface Sci.* **1999**, *212*, 443.
(24) Lee, E.; Chih, M. H.; Hsu, J. P. *J. Phys. Chem. B* **2001**, *105*, 747.
(25) Carrique, F.; Arroyo, F. J.; Delgado, A. V. *J. Colloid Interface Sci.* **2002**, *252*, 126.
(26) Levine, S.; Neale, G. H.; Epstein, N. *J. Colloid Interface Sci.* **1976**, *57*, 424.
(27) Ohshima, H. *J. Colloid Interface Sci.* **1998**, *208*, 295.
(28) Ohshima, H. *J. Colloid Interface Sci.* **1997**, *195*, 137.
(29) Lee, E.; Yen, F. Y.; Hsu, J. P. *J. Phys. Chem. B* **2001**, *105*, 7239.
(30) Hsu, J. P.; Lee, E.; Yen, F. Y. *J. Phys. Chem. B* **2002**, *106*, 4789.
(31) Carrique, F.; Arroyo, F. J.; Jiménez, M. L.; Delgado, A. V. *J. Chem. Phys.* **2003**, *118*, 1945.
(32) Ruiz-Reina, E.; Carrique, F.; Rubio-Hernández, F. J.; Gómez-Merino, A. I.; García-Sánchez, P. *J. Phys. Chem. B* **2003**, *107*, 9528.
(33) Ruiz-Reina, E.; Garcia-Sanchez, P.; Carrique, F. *J. Phys. Chem. B* **2005**, *109*, 5289.
(34) Carrique, F.; Garcia-Sanchez, P.; Ruiz-Reina, E. *J. Phys. Chem. B* **2005**, *109*, 24369.
(35) Ohshima, H.; Dukhin, A. S. *J. Colloid Interface Sci.* **1999**, *212*, 449.
(36) Dukhin, A. S.; Ohshima, H.; Shilov, V. N.; Goetz, P. J. *Langmuir* **1999**, *15*, 3445.
(37) Zholkovskij, E. K.; Masliyah, J. H.; Shilov, V. N.; Bhattacharjee, S. *Adv. Colloid Interface Sci.* **2007**, *279*, 134–135.
(38) Happel, J. *J. Appl. Phys.* **1957**, *28*, 1288.
(39) Kuwabara, S. *J. Phys. Soc. Jpn.* **1959**, *14*, 527.
(40) O'Brien, R. W.; White, L. R. *J. Chem. Soc., Faraday Trans. 2* **1978**, *74*, 1607.
(41) Ohshima, H.; Healy, T. W.; White, L. R. *J. Chem. Soc., Faraday Trans. 2* **1983**, *79*, 1613.
(42) DeLacey, E. H. B.; White, L. R. *J. Chem. Soc., Faraday Trans. 2* **1981**, *77*, 2007.
(43) Shilov, V. N.; Zharkikh, N. I.; Borkovskaya, Y. B. *Colloid J.* **1981**, *43*, 434.
(44) Carrique, F.; Cuquejo, J.; Arroyo, F. J.; Jiménez, M. L.; Delgado, A. V. *Adv. Colloid Interface Sci.* **2005**, *118*, 43.
(45) Shampine, L. F.; Kierzenka, J. *Solving boundary value problems for ordinary differential equations in MATLAB with bvp4c*; The MathWorks, Inc., 2000; available at http://www.mathworks.com/bvp_tutorial.
(46) Schaefer, D. W. *J. Chem. Phys.* **1977**, *66*, 3980.
(47) Deggelmann, M.; Palberg, T.; Hagenbuchle, M.; Maier, E. E.; Krause, R.; Graf, C.; Weber, R. *J. Colloid Interface Sci.* **1991**, *143*, 318.
(48) Hessinger, D.; Evers, M.; Palberg, T. *Phys. Rev. E* **2000**, *61*, 5493.
(49) Ohshima, H. *Colloids Surf., A* **2003**, *222*, 207.
(50) Pashley, R. M.; Rzechowicz, M.; Pashley, L. R.; Francis, M. J. *J. Phys. Chem. B* **2005**, *109*, 1231.

JP904421W